Available online at www.sciencedirect.com
SCIENCE DIRECT®
Journal of Sound and Vibration 260 (2003) 711–730
JOURNAL OF SOUND AND VIBRATION
www.elsevier.com/locate/jsvi

Non-trivial effect of fast vibration on the dynamics of a class of non-linearly damped mechanical systems

S. Chatterjee*, T.K. Singha, S.K. Karmakar

Department of Mechanical Engineering, Bengal Engineering College (Deemed University), P.O. Botanic Garden, Howrah-711103, West Bengal, India

Received 15 October 2001; accepted 8 May 2002

Abstract

The effect of very high-frequency excitation on the slow dynamics of a class of non-linearly damped mechanical oscillators is considered. Two different models of damping namely, piecewise linear and *p*th power damping are considered. Fast excitation is modelled as triangular, sinusoidal and random base excitation. The effect of fast excitation is theoretically analyzed using the method of direct partition of motion (MDPM) and direct simulation. The method of numerical averaging is also used, where damping characteristics or excitations are not amenable to analytical techniques. Fast excitation has the non-trivial effect of increasing and decreasing the low-velocity damping of hard and soft dampers, respectively. The effect of fast excitation on the transient and steady state slow dynamics of the system is investigated by direct numerical integration of the equation of motion.
© 2002 Elsevier Science Ltd. All rights reserved.

1. Introduction

Fast vibration refers to low-amplitude high-frequency excitation involving a time-period much shorter than the natural period of the system it is applied on. When a linear second order system is subjected to an excitation having a frequency very high compared to its natural frequency, no significant effect is observed in the dynamics at a time scale comparable to the natural period of the system. This is because of the fact that a second order linear system essentially acts as a band pass filter and filters out any frequency very much away from its natural frequency. However, recent research has revealed that non-linear systems, in general, cannot be treated as band pass

*Corresponding author.
E-mail address: shy@mech.becs.ac.in (S. Chatterjee).

0022-460X/03/$ - see front matter © 2002 Elsevier Science Ltd. All rights reserved.
PII: S0022-460X(02)00993-8

filters. Even a very high-frequency excitation may possibly have significant effect on the dynamics of non-linear systems at a time scale comparable to the natural time period (if any) of the system.

Use of high-frequency dither signal is well known to control engineers [1,2]. In control system applications, dither is used to smoothen out non-smooth non-linear characteristics (viz. dead zone, backlash, etc.) of various devices. Non-trivial effect of fast excitation is also known to dynamists. High-frequency support vibration is known to have stabilizing effect on inverted pendulum [3–9]. Theoretical and experimental research have been carried out to understand this stabilizing effect of fast support vibration (a form of parametric excitation) on the dynamics of inverted pendulum and related systems. Use of high-frequency vibration to minimize stick-slip motion of machine tool slide and low-velocity drives are reported in the literature [10,11]. When a body moves on a solid surface, stick-slip occurs at low-velocity of motion. Stick-slip motion is identified with the drooping characteristics of friction at low-velocity. When the solid surface vibrates with a very high-frequency in a direction normal/tangential to the slow velocity of the body, the negatively sloped friction force at low-velocity is flattened out and stick-slip is eliminated.

The effect of high-frequency vibration on non-linear elastic properties of material has been a great deal of interest in recent times. It is understood that new properties are possible to form by applying suitable high-frequency vibration [12–19]. The high-frequency excitation remains effectively unobserved in the response but its effect on system properties, as far as the slow dynamics are concerned, is tremendous and sometimes exotic too.

The non-trivial effect of fast vibration on the dynamics of non-linear systems, often called the fast vibration phenomena, has already found various practical applications [14]. Application of fast vibration in material transportation is reported in the literature [20–23].

The present paper deals with the effect of fast vibration on a class of non-linearly damped single-degree-of-freedom mechanical oscillators. Two different types of models of non-linear damping, namely piece-wise linear and pth power damping are considered. Fast excitation may be modelled by any periodic function having a short time period or a random signal with a PSD function concentrated near a frequency range far away from the natural frequency of the system. In the present theoretical investigation, triangular pulse periodic vibration, single harmonic sinusoid and high-frequency random excitations are considered as the models of fast excitation. The fast vibration is applied as base excitation to a single-degree-of-freedom non-linear oscillator. The method of direct partition of motion (MDPM) is used to analyze the effect of fast vibration on the slow dynamics of the system. Theoretical results reveal an average effect of high-frequency excitation on the slow dynamics of the system. Finally, direct numerical simulation of the equation of motion is carried out to validate the analytical results.

2. Theoretical analysis: method of direct partition of motion

A mathematical model of a single-degree-of-freedom oscillator with non-linear damping is depicted in Fig. 1. The oscillator is subjected to a high-frequency base excitation x_e. The non-dimensional equation of motion of the oscillator is written as

$$\ddot{X} + f_d(\dot{X}) + X = -\ddot{X}_e, \tag{2.1}$$

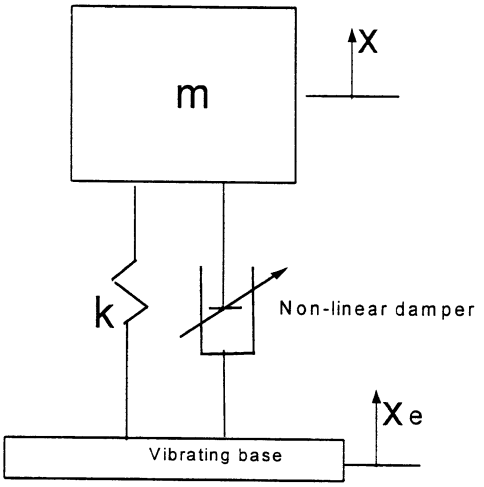

Fig. 1. Mathematical model of single-degree-of-freedom non-linearly damped mechanical oscillator with base excitation.

where dot (.) denotes differentiation with respect to non-dimensional time

$$\tau = \omega t.$$

Other non-dimensional quantities are described below:

$$\omega = \sqrt{\frac{k}{m}}, \quad X = \frac{y}{x_0}, \quad y = x - x_e, \quad X_e = \frac{x_e}{x_0},$$

where x_0 is an arbitrary length.

2.1. Model I: piece-wise linear damping with triangular pulse fast excitation

A piece-wise linear damping function is depicted in Fig. 2(a). The corresponding non-dimensional form of the damping function $f_d(.)$ is mathematically described as

$$f_d(\dot{X}) = h\{\mathrm{H}(V_0 - |\dot{X}|) + \lambda \mathrm{H}(|\dot{X}| - V_0)\} = hf(\dot{X}), \tag{2.2}$$

where

$$h = \frac{c}{m\omega} \quad \text{and} \quad V_0 = \frac{V_c}{\omega x_0}.$$

H(.) is the Heaviside step function defined as

$$\mathrm{H}(i) = \begin{cases} 1, & i >= 0, \\ 0, & i < 0. \end{cases}$$

For mathematical convenience, a triangular pulse periodic excitation is considered in this section. The displacement and the velocity time history of the base excitation are shown in Figs. 3(a) and (b), respectively. As the base excitation is a high-frequency low-amplitude vibration, one can

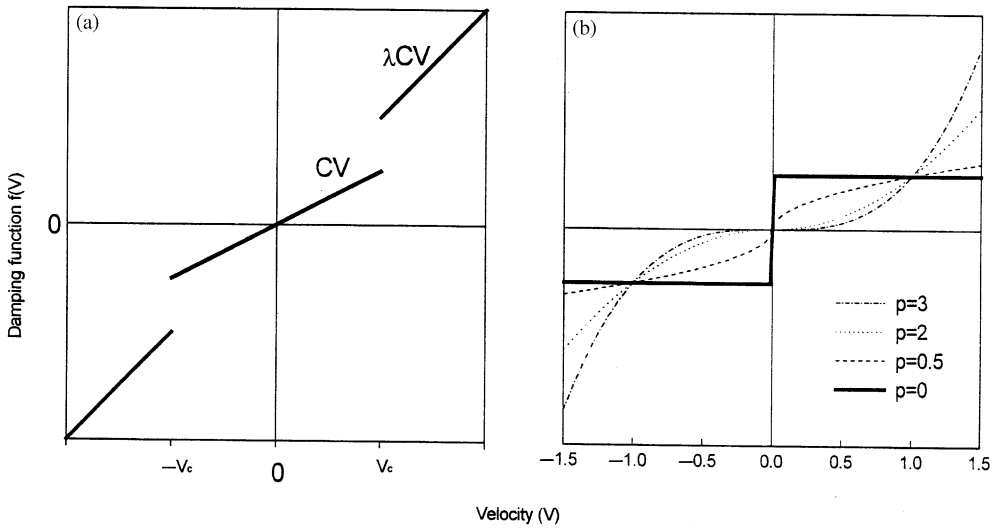

Fig. 2. Plots of non-linear damping characteristics considered in the present paper: (a) piecewise linear damping and (b) pth power damping.

assume that the time-period (T_0) and amplitude ($q/4$) are very small quantities. Thus,

$$T_0 \ll 1, \quad q \ll 1 \quad \text{and} \quad \frac{q}{T_0} = \mathrm{O}(1).$$

According to the MDPM [10,12], one can split the motion $X(\tau)$ into slow (Z) and fast (ϕ) components as follows:

$$X(\tau) = Z(\tau) + T_0\phi(\tau, T), \tag{2.3}$$

where

$$T = T_0^{-1}\tau$$

with

$$\langle \phi \rangle = T_0^{-1} \int_0^{T_0} \phi(\tau, T)\, \mathrm{d}T = 0 \tag{2.4}$$

One may note that in Eq. (2.3), the dynamics is described in two time scales τ and T. Figs. 3(c) and (d) depict the base excitation in time scale T. From Eq. (2.3) one obtains

$$\dot{X}(\tau) = \dot{Z}(\tau) + \phi' + T_0\dot{\phi}, \tag{2.5}$$

$$\ddot{X}(\tau) = \ddot{Z}(\tau) + \phi'' T_0^{-1} + 2\dot{\phi}' + T_0\ddot{\phi}, \tag{2.6}$$

where $'$ denotes differentiation with respect to time T.

Inserting (2.3), (2.5) and (2.6) into Eq. (2.1), one finally obtains

$$\phi'' = -T_0\{\ddot{Z} + 2\dot{\phi}' + f(\dot{Z} + \phi') + (Z + T_0\phi)\} - T_0\ddot{X}_e + \mathrm{O}(T_0^2) \tag{2.7}$$

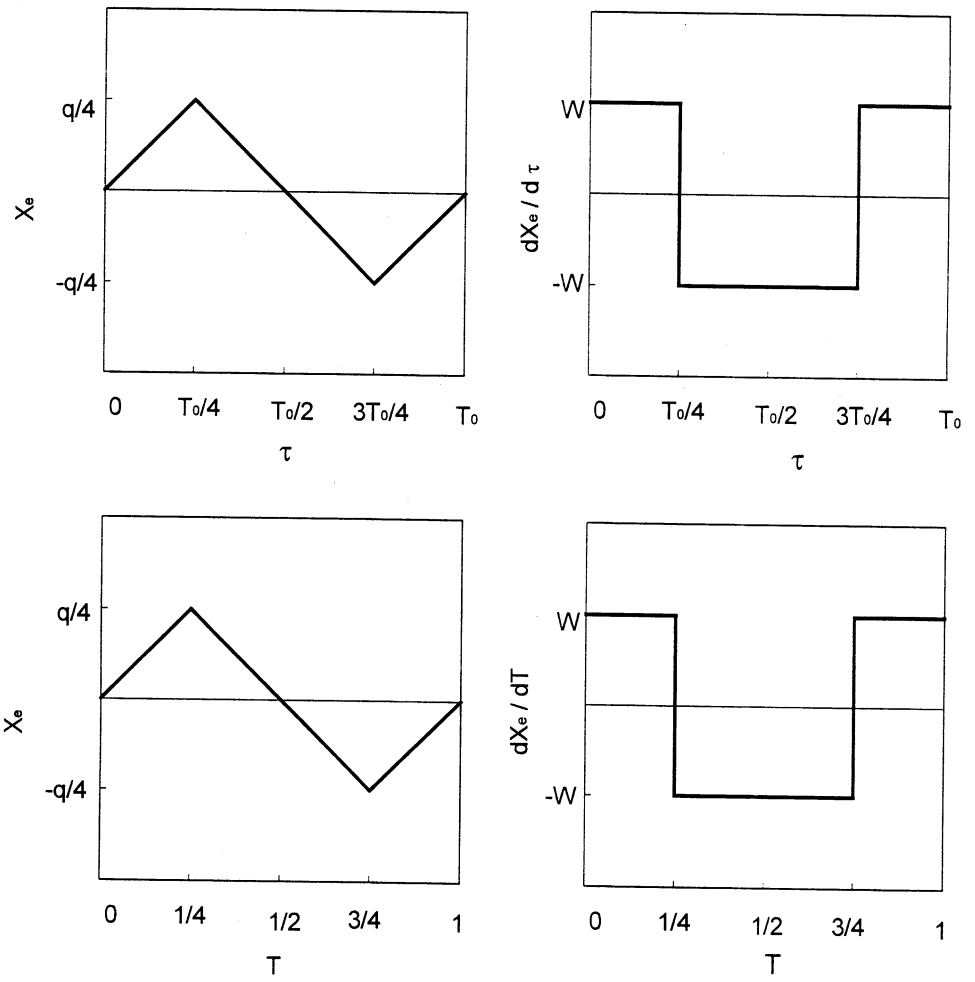

Fig. 3. Triangular pulse fast excitation and its derivative.

A first order form of Eq. (2.5) is given

$$\phi'' = -T_0 \ddot{X}_e. \tag{2.8}$$

Integrating Eq. (2.8) once, one obtains

$$\phi' = -T_0 \int \ddot{X}_e \, dT = -\int \ddot{X}_e \, d\tau = -\dot{X}_e. \tag{2.9}$$

From Eq. (2.9), one observes that the time history of ϕ' is similar to as shown in Fig. 3(c) only with a reverse sign.

Let

$$T_0^{-1} q = W. \tag{2.10}$$

Using Eq. (2.5), one finally obtains the slow dynamics of the system (in the time scale τ) by averaging Eq. (2.7) over a time-period T_0. The slow dynamics is given by

$$\ddot{Z} + h\langle f(\dot{Z} + \phi')\rangle + Z = 0. \tag{2.11}$$

Using the time history of ϕ' as described in Eq. (2.9), one obtains

$$\begin{aligned}\langle f(\dot{Z} + \phi')\rangle &= (\dot{Z} + W)\{\mathrm{H}(V_0 - |\dot{Z} + W|) + \lambda \mathrm{H}(|\dot{Z} + W| - V_0)\}/2 \\ &+ (\dot{Z} - W)\{\mathrm{H}(V_0 - |\dot{Z} - W|) + \lambda \mathrm{H}(|\dot{Z} - W| - V_0)\}/2.\end{aligned} \tag{2.12}$$

Let

$$W = \alpha V_0.$$

Two different cases, depending on the values of α, are discussed below.

Case I: $\alpha < 1$.

For $\alpha < 1$:

$$\begin{aligned}\langle f\rangle &= \dot{Z}, \quad \forall 0 < \dot{Z} < (1-\alpha)V_0, \\ \langle f\rangle &= \frac{\dot{Z}(1+\lambda) + W(\lambda - 1)}{2}, \quad \forall (1-\alpha)V_0 < \dot{Z} < (1+\alpha)V_0, \\ \langle f\rangle &= \lambda \dot{Z}, \quad \forall (1+\alpha)V_0 < \dot{Z} < \infty.\end{aligned} \tag{2.13}$$

Case II: $\alpha > 1$

For $\alpha > 1$:

$$\begin{aligned}\langle f\rangle &= \lambda \dot{Z}, \quad \forall 0 < \dot{Z} < (\alpha - 1)V_0, \\ \langle f\rangle &= \frac{\dot{Z}(1+\lambda) + W(\lambda - 1)}{2}, \quad \forall (\alpha-1)V_0 < \dot{Z} < (1+\alpha)V_0, \\ \langle f\rangle &= \lambda \dot{Z}, \quad \forall (1+\alpha)V_0 < \dot{Z} < \infty.\end{aligned} \tag{2.14}$$

Eqs. (2.13) and (2.14) express $\langle f\rangle$ only for positive values of $\dot{Z}$. However, one should note that $\langle f\rangle$ is symmetric function of $\dot{Z}$.

2.1.1. *Results and discussions on model I*

From the above analysis, it is understood that the effect of fast vibration on the slow dynamics of the system, originally described by non-autonomous differential equation (2.1), is effectively analyzed by an approximate autonomous differential Eq. (2.11). One can observe from Eq. (2.11) that high-frequency base excitation influences only the damping characteristics of the system at a time scale comparable to the natural period of it.

Depending on the values of λ, the damper may be soft ($\lambda < 1$) or hard ($\lambda > 1$). Therefore, two different cases are considered here. The effect of fast vibration on soft dampers is depicted in Figs. 4(a) and (b) for two different values of α. The effect of fast vibration on hard dampers is depicted in Figs. 4(c) and (d). For the type of system and excitation considered here, damping force may be described in three velocity ranges (a function of excitation strength W) viz. low, medium and high. In the present context, as one is interested only in slow dynamics, the low-velocity damping characteristics is of importance. From Figs. 4(a)–(d) few general conclusions may be drawn and these are in order.

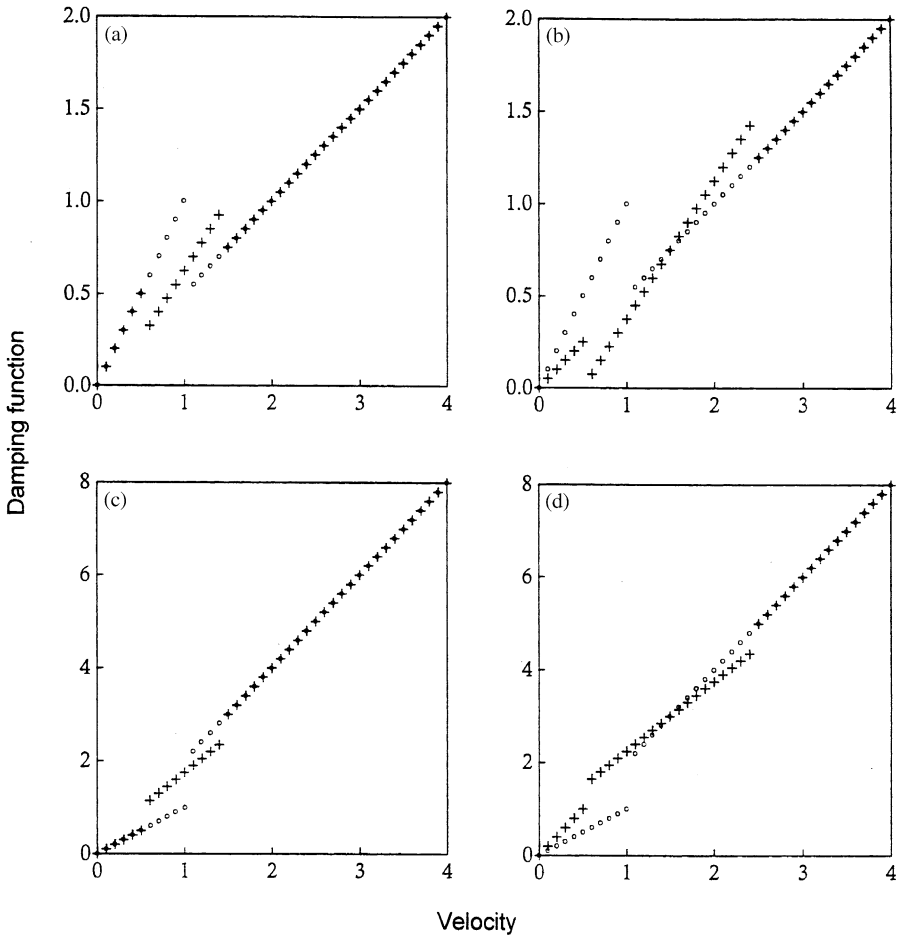

Fig. 4. Effect of fast vibration on piecewise linear damping: +, with fast vibration; ○, without fast vibration. $V_0 = 1$. (a) $\lambda = 0.5$, $\alpha = 0.5$; (b) $\lambda = 0.5$, $\alpha = 1.5$; (c) $\lambda = 2.0$, $\alpha = 0.5$; (d) $\lambda = 2.0$, $\alpha = 1.5$.

When damper characteristics is soft ($\lambda < 1$) and fast excitation is weak ($\alpha < 1$), the very low-velocity and the very high-velocity damping remains unchanged and only the medium-velocity damping is influenced (Fig. 4(a)). With the increase of the strength of excitation (α), the range of influence extends both in the low- and high-velocity zone.

When the damper characteristics is soft and the fast excitation is strong ($\alpha > 1$), both the low- and medium-velocity damping is affected. However, the very high-velocity damping remains unchanged. As seen from Fig. 4(b), the low-velocity damping is reduced by the fast excitation. The low-velocity damping decreases with the increase of the strength of excitation and the range of influence extends towards the higher velocity. The very high-velocity range, where damping remains unchanged, is shifted towards higher velocity.

When the damper characteristics is hard and the excitation is weak, as shown in Fig. 4(c), conclusions are the same as in the case of soft damper and weak excitation.

When the damper is hard and the excitation is strong, as shown in Fig. 4(d), the low-velocity damping increases and the high-velocity damping remains unchanged. The low-velocity damping increases with the increase of the strength of excitation and the range of influence extends towards higher velocity. The high-velocity range of non-influence is shifted towards higher velocity.

2.2. Model II: pth power damping with triangular pulse fast excitation

With the non-linear damper obeying pth power damping law (Fig. 2(b)) the damping term $f_d(.)$ in Eq. (2.1) assumes the following form:

$$f_d(\dot{X}) = hf(\dot{X}),$$

where

$$f(\dot{X}) = \dot{X}|\dot{X}|^{p-1} \tag{2.15}$$

and

$$h = \frac{Cx_0^{p-1}\omega^{p-2}}{m}.$$

It is to be noted here that pth power law models a wide class of non-linear damping. Theoretically p can assume any value. However, for the present analysis p is restricted to be semi-positive (stable systems). $p = 0$ signifies Coulomb's dry friction damping, where as $p = 1$ and 2 signify quadratic and cubic damping, respectively.

Following the same analysis as described in the case of model I, one arrives at the following equation describing the slow dynamics of the system:

$$\ddot{Z} + h\langle f(\dot{Z} + \phi')\rangle + Z = 0, \tag{2.16}$$

where the shape of ϕ' is as described earlier in Eq. (2.9).

One obtains the average damping characteristic $\langle f \rangle$ as given below:

$$\langle f(\dot{Z} + \phi')\rangle = \frac{h[(\dot{Z} + W)|\dot{Z} + W|^{p-1} + (\dot{Z} - W)|\dot{Z} - W|^{p-1}]}{2}. \tag{2.17}$$

Average damping functions for four different cases of p are discussed below:

Case I: p = odd integer

$$\langle f \rangle = \sum_{r=0,2,4}^{p-1} \binom{p}{r} \dot{Z}^{p-r} W^r. \tag{2.18}$$

Case II: p = even integer

$$\langle f \rangle = \frac{\{\mathrm{sgn}(\dot{Z} + W)(\dot{Z} + W)^p + \mathrm{sgn}(\dot{Z} - W)(\dot{Z} - W)^p\}}{2}.$$

Thus,

$$\langle f \rangle = \sum_{r=1,3}^{p-1} \binom{p}{r} \dot{Z}^{p-r} W^r, \quad \forall 0 < |\dot{Z}| < W,$$

$$\langle f \rangle = \sum_{r=0,2,4}^{p} \binom{p}{r} \dot{Z}^{p-r} W^r, \quad \forall W < |\dot{Z}| < \infty. \tag{2.19}$$

Case III: $p = 0$

$$\langle f \rangle = \frac{\{\mathrm{sgn}(\dot{Z} + W) + \mathrm{sgn}(\dot{Z} - W)\}}{2}.$$

Thus

$$\langle f \rangle = 0, \quad \forall 0 < |\dot{Z}| < W,$$

$$\langle f \rangle = 1, \quad \forall W < |\dot{Z}| < \infty. \tag{2.20}$$

Case IV: $p =$ positive fraction

$$\langle f \rangle = \sum_{r=1,3,\ldots}^{\infty} \frac{p(p-1)\ldots\ldots(p-r+1)}{r!} \dot{Z}^r W^{p-r}. \tag{2.21}$$

2.2.1. *Results and discussions on model II*

As in the case of model I, here also the effect of fast vibration is described effectively by an autonomous Eq. (2.16). For easy understanding of the effect of fast vibration on low-velocity damping, few typical values of the damping involution p are considered below:

For $p = 2$:

$$\begin{aligned} \langle f \rangle &= 2W\dot{Z}, \forall 0 < |\dot{Z}| < W \\ &= (\dot{Z}^2.. + W^2)\mathrm{sgn}(\dot{Z}), \quad \forall W < |\dot{Z}| < \infty. \end{aligned} \tag{2.22}$$

For $p = 3$:

$$\langle f \rangle = (3W^2\dot{Z} + \dot{Z}^3). \tag{2.23}$$

For $p = 5$:

$$\langle f \rangle = (\dot{Z}^5 + 10W^2\dot{Z}^3 + 5W^4\dot{Z}) \tag{2.24}$$

It is observed from Eqs. (2.22)–(2.24) that as a result of fast excitation, original pth power damping function, expressed as monomial functions of velocity (for unidirectional velocity), changes to polynomial functions containing lower ($<p$) order terms of velocity. Consequently, damping increases at low-velocity.

Non-linear dampers with pth power damping law can be classified as soft and hard dampers depending on the values of p. Soft dampers are modelled by $p < 1$ and hard dampers are modelled by $p > 1$. The effect of fast vibration on soft and hard pth power dampers is best understood from Figs. 5(a)–(d), where average damping function $\langle f \rangle$ are plotted for different values of p (3, 2, 0.5, 0). From the above analysis and Figs. 5(a)–(d) few general conclusions can be made regarding the effect of fast vibration on pth power damping.

Hard dampers ($p > 1$) produce higher damping force at high velocity. However, damping force is generally very poor at low-velocity. Fast vibration, as shown in Figs. 5(a) and (b), increases low-velocity damping of hard dampers.

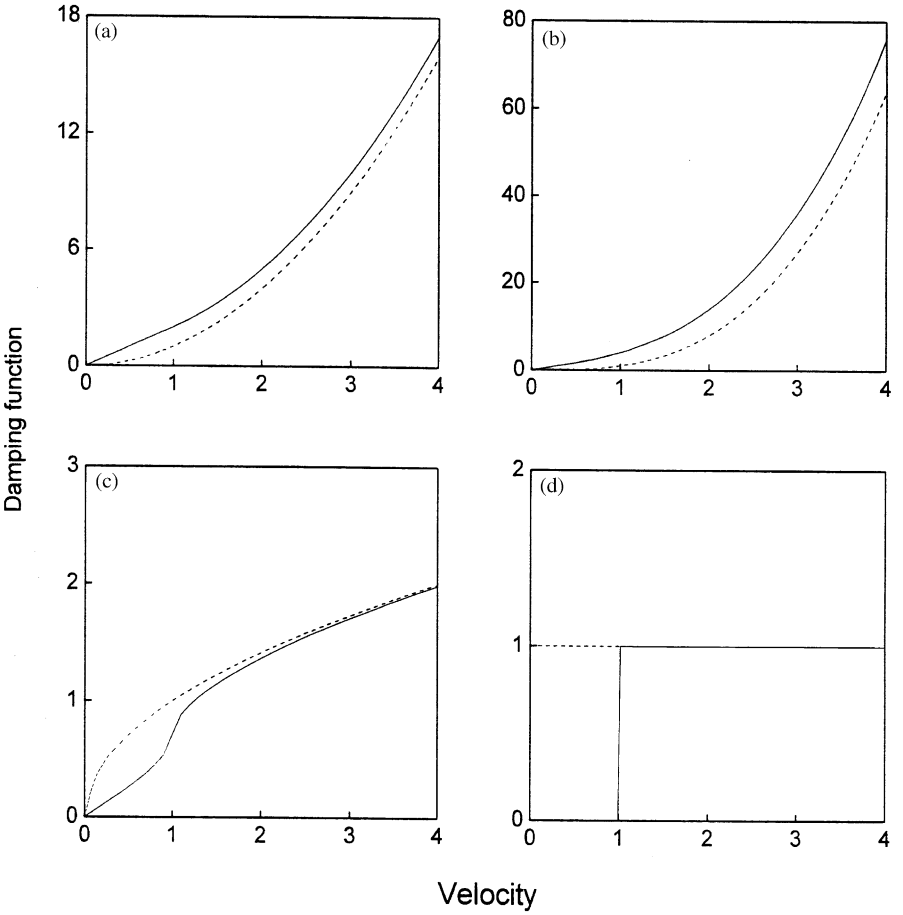

Fig. 5. Effect of fast vibration on pth power damping. ——, with fast vibration; ----------, without fast vibration. $W = 1$. (a) $p = 2$, (b) $p = 3$, (c) $p = 0.5$, (d) $p = 0$.

However, the low-velocity damping of soft dampers ($p<1$) is reduced by fast excitation. The effect of fast excitation on soft dampers is shown in Figs. 5(c)–(d). As mentioned earlier, $p = 0$ corresponds to friction damping and represents an extreme case of soft damping characteristics.

2.3. Model III: pth power damping with sinusoidal fast excitation

In case of pth power damper with harmonic fast excitation $x_e = Q\sin(\omega_f t)$, equation of motion assumes the following form

$$\ddot{X} + h\dot{X}|\dot{X}|^{p-1} + X = q\Omega^2 \sin(\Omega\tau), \tag{2.25}$$

where

$$h = \frac{Cx_0^{p-1}\omega^{p-2}}{m}$$

and

$$q = Q/x_0, \quad \Omega = \omega_f/\omega.$$

Using the same technique as elaborated in previous sections, one obtains an equivalent autonomous equation

$$\ddot{Z} + h\langle f(\dot{Z} + \phi')\rangle + Z = 0. \tag{2.26}$$

Using Eq. (2.9) one obtains

$$\phi' = -q\Omega\cos(\Omega\tau). \tag{2.27}$$

Thus, effective damping function is given by

$$\langle f\rangle = \frac{1}{2\pi}\int_0^{2\pi}(\dot{Z} - q\Omega\cos(\Omega\tau))|\dot{Z} - q\,\Omega\cos(\Omega\tau)|^{p-1}\,\mathrm{d}(\Omega\tau). \tag{2.28}$$

Now depending on the values of p, three different cases are considered below:

Case I: $p =$ odd integer

$$\langle f\rangle = \frac{1}{2\pi}\sum_{r=0,2,4}^{p-1}\binom{p}{r}(q\Omega)^r 2\sqrt{\pi}\frac{\Gamma((r+1)/2)}{\Gamma((r+2)/2)}\dot{Z}^{p-r}. \tag{2.29}$$

For example, when $p = 3$, the effective damping function becomes

$$\langle f\rangle = \dot{Z}^3 + \tfrac{3}{2}(q\Omega)^2\dot{Z}. \tag{2.30}$$

Case II: Quadratic damping ($p = 2$)

$$\begin{aligned}\langle f\rangle &= \frac{1}{2\pi}\{(2\pi - 4\theta_1)(\dot{Z}^2 + q^2\Omega^2/2) + 6q\Omega|\dot{Z}|\sin(\theta_1)\}\mathrm{Sgn}(\dot{Z}), \quad \forall 0 \leqslant |\dot{Z}| \leqslant q\Omega,\\ \langle f\rangle &= (\dot{Z}^2 + q^2\Omega^2/2)\mathrm{Sgn}(\dot{Z}), \quad \forall 0 \leqslant |\dot{Z}| \leqslant \infty.\end{aligned} \tag{2.31}$$

with

$$\theta_1 = \cos^{-1}\left(\frac{|\dot{Z}|}{q\Omega}\right)$$

Case III: friction damping ($p = 0$)

$$\begin{aligned}\langle f\rangle &= \left\{1 - \frac{2}{\pi}\cos^{-1}\left(\frac{|\dot{Z}|}{q\Omega}\right)\right\}\mathrm{Sgn}(\dot{Z}), \quad \forall 0 \leqslant |\dot{Z}| \leqslant q\Omega,\\ \langle f\rangle &= \mathrm{Sgn}(\dot{Z}), \quad \forall q\Omega \leqslant |\dot{Z}| \leqslant \infty.\end{aligned} \tag{2.32}$$

2.3.1. *Results and discussions on model III*

From Eqs. (2.29)–(2.32) it is obvious that harmonic fast excitation modifies the low-velocity damping in a similar fashion as discussed in case of model II. Effective damping functions are shown in Figs. 6(a)–(c) for $p = 3$, 2 and 0.

One may note that analytical results are difficult to obtain for even integer (> 2) and positive fractional values of p as well as arbitrarily complicated damping characteristics and fast

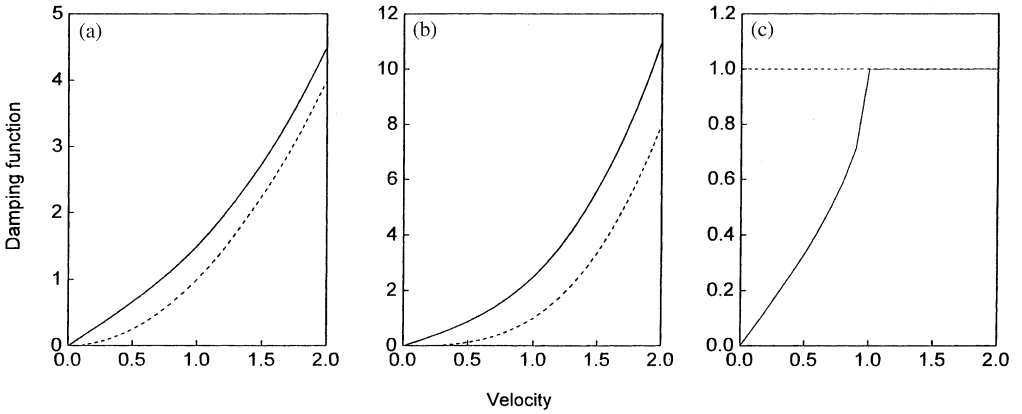

Fig. 6. Effect of harmonic fast vibration on pth power damping. ——, with fast vibration; ---------, without fast vibration. $q\Omega = 1$. (a) $p = 2$, (b) $p = 3$, (c) $p = 0$.

excitation. In such cases, numerical techniques may be adopted to compute the damping function. In what follows a numerical method is described to compute the average damping function in presence of fast excitation.

3. Method of numerical averaging: random excitation

In the above analysis, fast vibration has been taken to be either harmonic or triangular pulse type. However, when damping function is complicated and fast excitation is complex it is difficult to obtain a closed-form solution of the problem. In this section, a numerical method (the method of numerical averaging (MNA)) for computing effective damping function is discussed.

Effective damping function is computed according to the following equation:

$$\langle f \rangle = \frac{1}{T}\int_0^T f(V + e(t))\,\mathrm{d}t, \tag{3.1}$$

where V is the slow velocity of motion, $e(t)$ is the velocity of fast excitation and T is the sample period of $e(t)$. The value of T is of the same order of magnitude as natural period of the system. Average damping function $\langle f \rangle$ can be computed analytically for some simple cases. One such example is discussed below.

For the dampers following pth power (where p is odd integer) damping law, one computes the average damping function as

$$\langle f \rangle = \left[\binom{p}{r} V^{p-r}\frac{1}{T}\int_0^T \{e(t)\}^r\,\mathrm{d}t\right]. \tag{3.2}$$

For $p = 3$, one obtains

$$\langle f \rangle = V^3 + 3V\sigma^2, \tag{3.3}$$

where

$$\sigma^2 = \frac{1}{T}\int_0^T e^2 \, \mathrm{d}t$$

represents the variance of the samples of the random signal over time period T.

For even integer and fractional values of p, computation of the average in a closed form is difficult. In such cases, the method of numerical averaging may be used to calculate effective damping functions. In what follows the method of numerical averaging is described in details.

The effective damping is numerically computed according to Eq. (3.1). A random signal $e^*(t)$ is constructed by assigning random numbers (uniformly distributed between -1 and 1) to small uniform sampling intervals (order of magnitude few order less than the natural period of the system). In the present paper, a sampling interval 0.0001 and a total sample period 1 are used. The random fast excitation $e(t)$ is constructed by further processing $e^*(t)$ through a band pass filter with a pass band frequency lying between 1000 and 5000 Hz. The filtered signal $e(t)$, thus formed, is shown in Fig. 7(a) and (b) and used for numerical averaging. The random signal $e(t)$ is added to V (a constant parameter) to compute $f(V + e(t))$ and sampled at regular time interval 0.01 over a time period 1. The arithmetic average of the collected samples represents the value of the damping function $\langle f \rangle$ at velocity V. This procedure may be repeated for a number of different values of V and finally the effective damping function is graphically constructed. This procedure may also be

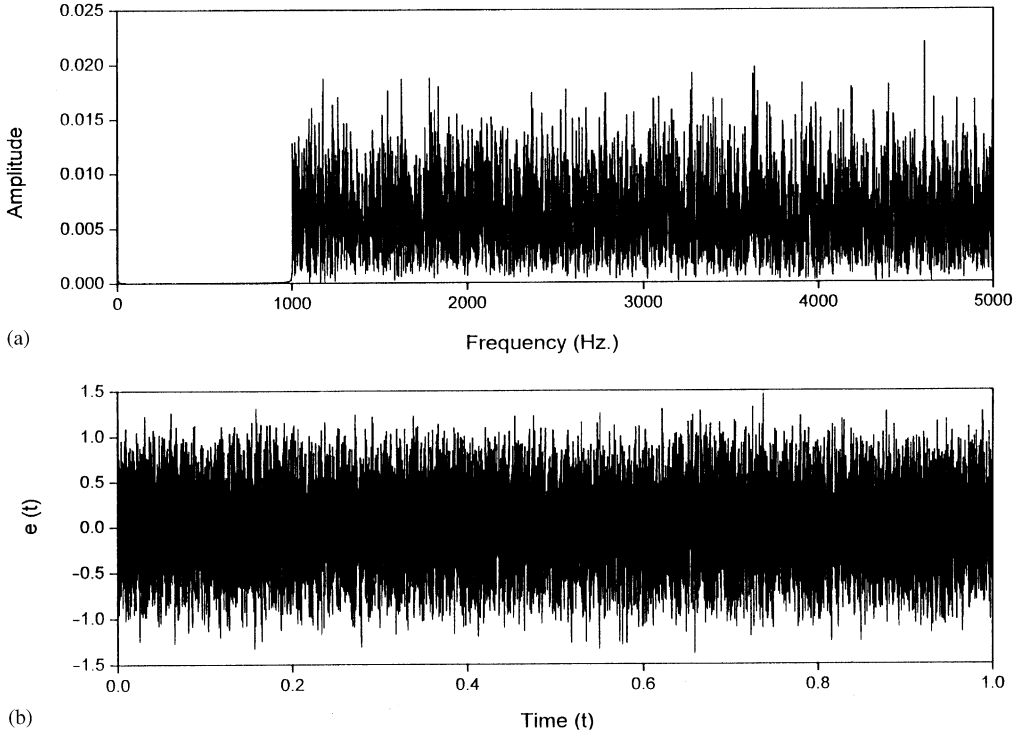

Fig. 7. Random high-frequency velocity excitation $e(t)$ used for numeric averaging: (a) FFT plot and (b) time history.

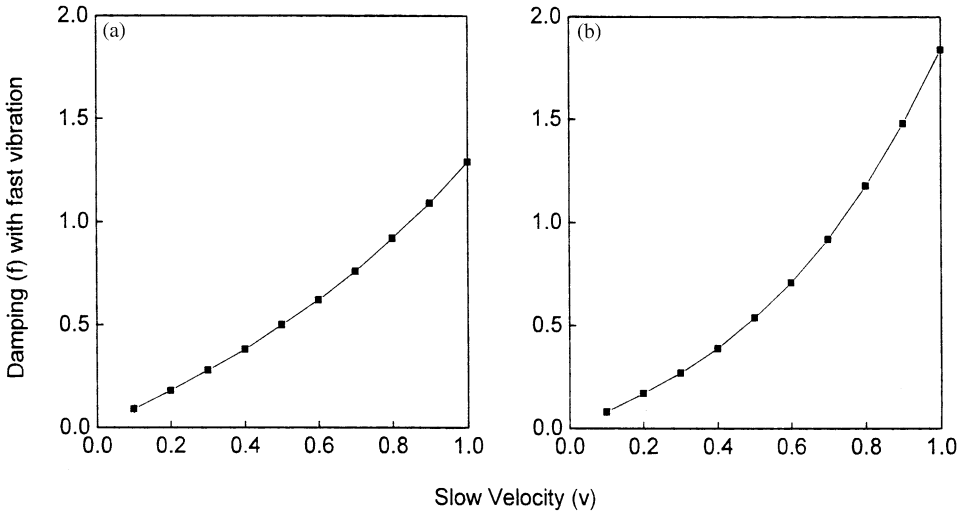

Fig. 8. Effective damping function plot obtained by MNA: (a) $p = 2$ and (b) $p = 3$.

applied for periodic excitation without any difficulty. Results of the numerical averaging are described in the next section.

3.1. Results and discussions on the MNA

As analytical result is available for cubic damping ($p = 3$), this value of p is chosen for the validation of the method of numerical averaging. The simulated damping function is shown in Fig. 8(a). By fitting the data by a polynomial curve, one obtains the expression of the damping function as

$$\langle f \rangle = 0.9947V^3 + 0.8V. \tag{3.4}$$

Comparing Eq. (3.4) with (3.3) and noting that the sample variance of the random signal $e(t)$ is 0.263, one proves the validity of the numerical averaging method. Fig. 8(b) shows the simulated damping function for quadratic damping ($p = 2$). Here damping function is evaluated as

$$\langle f \rangle = 0.5511V^2 + 0.7207V. \tag{3.5}$$

For integer values of p, one can naturally expect to obtain polynomial expressions of the effective damping functions at low-velocity. In order to have a good estimate of low-velocity damping for other complex damping characteristics, it is pertinent to compute only the slope of the effective damping function near zero velocity ($V = 0$).

4. Direct numerical simulation

From the expressions of the effective damping functions obtained in Sections 2 and 3, it may be concluded that the low-velocity damping of hard dampers increases due to fast vibration. On the

other hand, the low-velocity damping of soft dampers decreases due to fast excitation. In support of the above conclusions, in this section, direct numerical integration of equation of motion (2.25) is carried out to compute the response of the system under high-frequency harmonic excitation. Numerical integration of Eq. (2.25) is carried out using the Runge–Kutta–Merson algorithm with adaptive step size control (a NAG library subroutine). As only the slow dynamics of the system is of major concern, the integrated results are sampled at a very low frequency (sampling interval 0.01 is used). Transient response of the system, in terms of the absolute displacement $(X + X_e)$ of the vibrating mass, is computed. The effect of fast excitation on the transient response of the system with hard damping ($p = 2$) is shown in Fig. 9. The transient response of the system with soft damping ($p = 0.5$) is shown in Fig. 10.

It is already observed that the strength of the fast excitation, defined as the product of the excitation amplitude and the frequency plays the dominant role in the expressions of the effective damping. According to the assumptions of the MDPM, $\Omega \gg 1$ and $q\Omega \sim O(1)$. This is maintained in numerical simulation by choosing a very small value of q and a very large value of Ω· In Figs. 9 and 10, Ω is kept constant at 1000 and q is varied to change the strength of excitation. It may be mentioned that the effect of $\Omega = 1000$ and $q = 0.001$ is the same as that of $\Omega = 10000$ and $q = 0.0001$. Theoretically, larger the values of Ω better should be the matching between the results obtained from Eqs. (2.25) and (2.26). However, numerical simulation of Eq. (2.25) becomes difficult for very high values of Ω· From Fig. 9 it is observed that the rate of decay of vibration increases with q. This validates the conclusion that the low-velocity damping of hard dampers increases due to fast excitation. From Fig. 10, it is observed that the rate of decay of vibration decreases as q increases. This is also consistent with the conclusion that the low-velocity damping of soft dampers decreases due to fast excitation.

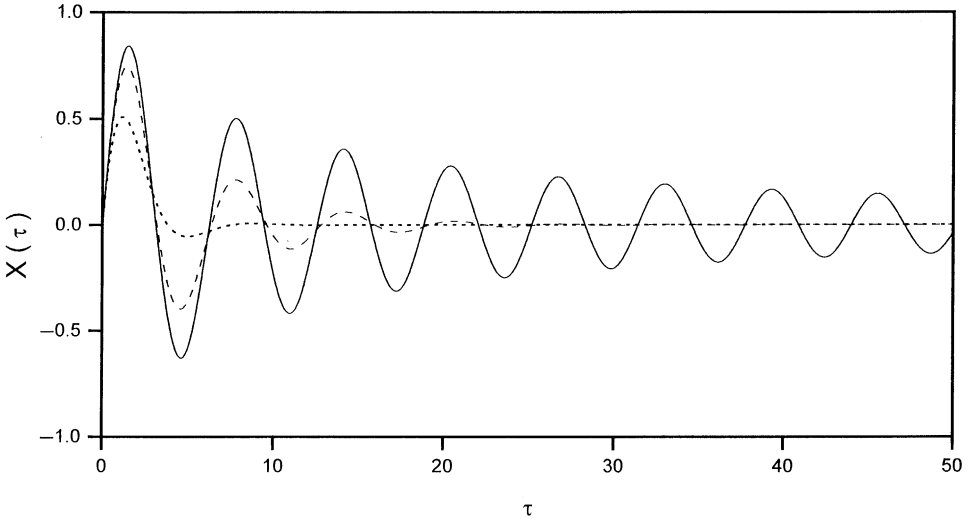

Fig. 9. Effect of fast vibration on the transient response of a single-degree-of-freedom system with pth power damping. $p = 2$. ——, without fast vibration, - - -, with fast vibration ($q = 0.001$, $\Omega = 1000$); ------, with fast vibration ($q = 0.003$, $\Omega = 1000$).

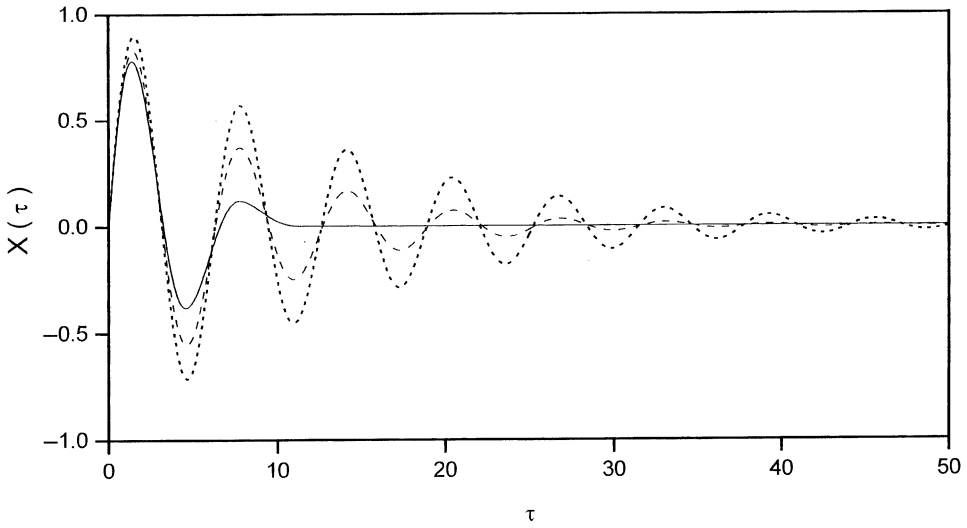

Fig. 10. Effect of fast vibration on the transient response of a single-degree-of-freedom system with pth power damping. $p = 0.5$, ——, without fast vibration, - - - with fast vibration ($q = 0.001$, $\Omega = 1000$); - - - - - with fast vibration ($q = 0.003$, $\Omega = 1000$).

The theoretical analysis leads to the conclusions that Eq. (2.26) faithfully represents the slow dynamics of the system described by Eq. (2.25) and the slow response of the system is exclusively a function of $q\Omega$ irrespective of the individual values of q and $\Omega\cdot$ To demonstrate this numerically, the excitation is assumed to contain a low-frequency harmonic component of the form $\sin(\tau)$ along with the usual fast vibration. Thus, Eqs. (2.25) and (2.26) assume the following forms as given by

$$\ddot{X} + h\dot{X}|\dot{X}|^{p-1} + X = q\Omega^2 \sin(\Omega\tau) + \sin(\tau), \tag{4.1}$$

$$\ddot{Z} + h\langle f(\dot{Z} + \phi')\rangle + Z = \sin(\tau). \tag{4.2}$$

Eqs. (4.1) and (4.2) are numerically integrated for the following set of values:

Set I: ($q = 0.003$, $\Omega = 1000$); $q\Omega = 3$;
Set II: ($q = 0.0001$, $\Omega = 3000$); $q\Omega = 3$.

Numerical results are shown in Figs. 11(a) and (b), from which it is observed that the steady state responses are the same for the systems governed by Eqs. (4.1) and (4.2). Responses are also exactly equal for the data sets II and I.

According to the theory of MDPM, autonomous equation (2.26) approximates the slow behaviour of the original system governed by Eq. (2.25). Though the theory of MDPM assumes that $\Omega \gg 1$, the theory does not provide any clear indication as for what range of values of Ω Eq. (2.26) faithfully represents the slow dynamics of the system. Thus, it is pertinent to look into

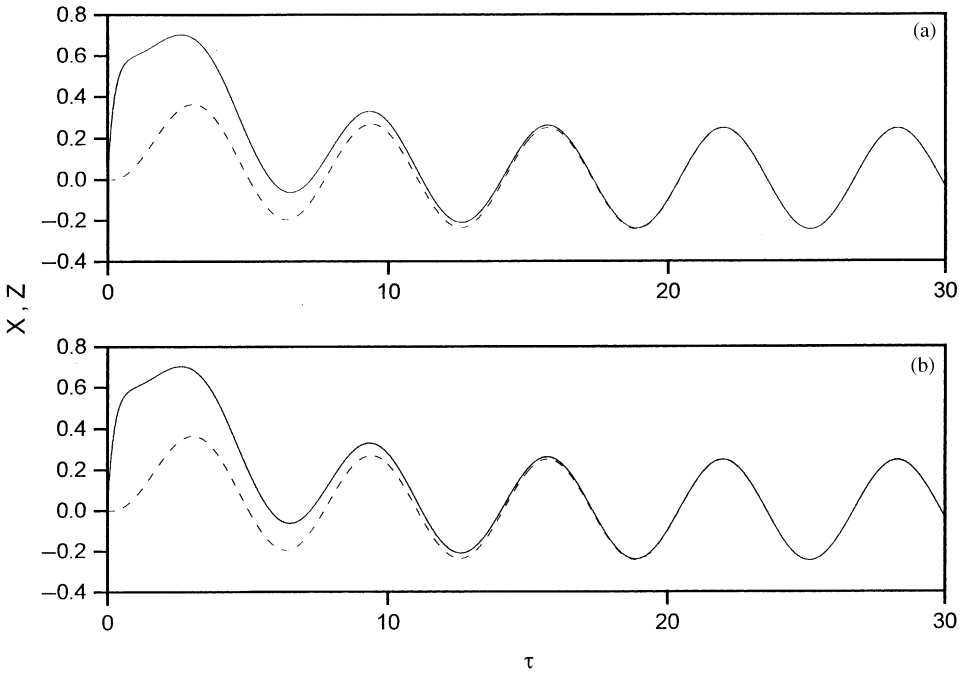

Fig. 11. Comparison of actual response X (----) and average theretical response Z (——) obtained from MDPM: (a) $q = 0.001$, $\Omega = 3000$ and (b) $q = 0.003$, $\Omega = 1000$.

the effect of the individual values of q and Ω, while keeping $q\Omega$ constant, on the slow response of the system. For this, Eqs. (4.1) and (4.2) are numerically integrated for a third data set.

Set III: ($q = 0.03$, $\Omega = 100$); $q\Omega = 3$.

Corresponding slow response of the system is shown in Fig. 12. In Fig. 12, one may observe prominent presence of the high-frequency component in the response of the original system given by Eq. (4.1). The response the system governed by the average Eq. (4.2) follows the average trend of the actual response. However, it is already observed that the high-frequency component is not prominently present in the response shown in Figs. 11(a) and (b), where lower values of q and higher values of Ω are used. A theoretical explanation of this behaviour is given below. The frequency (Ω) of fast excitation being far away from the natural frequency of the system (unity in the present case), one may approximately calculate the amplitude (A_{hf}) of high-frequency component of the response of the system (Eq. (4.1)) as

$$A_{hf} \approx \frac{q\Omega^2}{1-\Omega^2} \approx q = \frac{q\Omega}{\Omega} = \frac{C_0}{\Omega}, \quad \forall \Omega \gg 1. \tag{4.3}$$

where

$$C_0 = q\Omega.$$

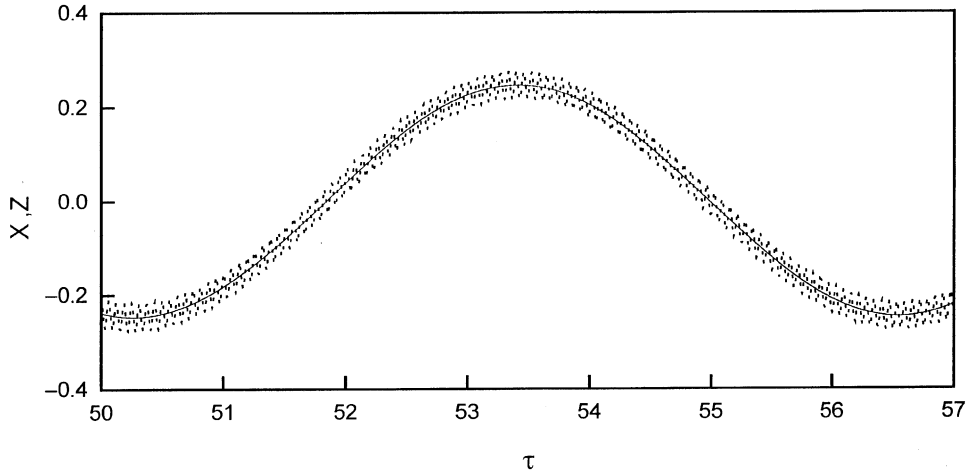

Fig. 12. Comaprison of actual response (X) and average response (Z). $h = 0.3$, $q = 0.03$, $\Omega = 100$. ———, average response (Z); - - - - - - -, actual response (X).

Thus for a fixed value of $q\Omega$, the amplitude of high-frequency component of the response is inversely proportional to the frequency of fast excitation and approximately equal to q. Therefore, the first approximation of the MDPM (which suppresses the high-frequency component in the response) is accurate only for infinitely large values Ω and infinitesimally small values of q. As in practice and also in numerical simulation both q and Ω are finite, the high-frequency component (approximately equal to q) is present in the response.

5. Conclusions

The effect of very high-frequency low-amplitude vibration on a class of non-linearly damped mechanical oscillator is discussed. Two different models of the damper, namely piecewise linear damping and pth power models are considered. Fast vibration is modelled as triangular pulse periodic excitation, harmonic and high-frequency random excitation. High-frequency excitation is shown to have a major influence on the damping characteristics of the damper, particularly in the low-velocity range. Effective damping functions are constructed either analytically or numerically. The method of direct partition of motion is used to obtain analytical solution of the problem for triangular and harmonic excitations. The method of numerical averaging is used, where analytical solutions are difficult to obtain. From the analysis, it is concluded that the low-velocity damping of hard damper increases and low-velocity damping of soft damper decreases due to fast vibration. Direct numerical simulation of the system is performed to validate the above conclusions. It is found that the strength of excitation, defined as the product of amplitude and frequency of excitation, decides the value of the average effective damping irrespective of the individual values of the amplitude and frequency of fast excitation.

Finally, it is to mention that the results of the present study have an immense practical importance. Fast vibration may be used as a technique to control damping characteristics of

non-linear dampers in active and semi-active control schemes of dynamical systems. For practical implementation of this concept, further experimental investigations are required in this direction. However, at this point a note of caution may be issued for those experimentalists who are involved in modelling damping characteristics of non-linear systems. Experiment is generally performed to model damping in a frequency range around lower order natural frequencies, as damping is believed to play a dominant role in that range of frequencies. Due to the presence of any unobserved high-frequency excitation, there is every possibility to obtain only an apparent damping model that may be very much different from the actual one.

Acknowledgements

The authors gratefully acknowledge the valuable comments of the referees (unknown) of this paper.

References

[1] P.A. Cook, Nonlinear Dynamical Systems, Prentice-Hall International, Englewood Cliffs, NJ, 1986.
[2] R.E. Bellman, J. Bentsman, S.M. Meerkov, Vibrational control of nonlinear systems: vibrational stabilization (1) vibrational controllability and transient behaviour (2), IEEE Transactions on Automatic Control AC-31 (8) (1986) 710–724.
[3] V.N. Chelomey, On possibility of increasing stability of elastic systems by vibration, Doklady AN SSSR 110 (3) (1956) 341–344.
[4] V.N. Chelomey, Dynamic stability upon high-frequency parametric excitation, Soviet Physics Doklady 26 (1981) 390–392.
[5] V.N. Chelomey, Mechanical paradoxes caused by vibrations, Soviet Physics Doklady 28 (1983) 387–390.
[6] J.S. Jensen, Nonlinear dynamics of the follower-loaded double pendulum with added support excitation, Journal of Sound and Vibration 215 (1998) 125–142.
[7] J.M. Schmitt, P.V. Bayly, Bifurcations in the mean angle of a horizontally shaken pendulum: analysis and experiment, Nonlinear Dynamics 15 (1998) 1–14.
[8] S. Weibel, T.J. Kepler, J. Baillieul, Global dynamics of a rapidly forced cart and pendulum, Nonlinear Dynamics 13 (1997) 131–170.
[9] J.J. Thomsen, D.M. Tcherniak, Chelomei's pendulum explained, Proceedings of the Royal Society of London A 457 (2012) (2001) 1889–1913.
[10] W. Oppelt, A historical review of autopilot development, research, and theory in Germany, Journal of Dynamic Systems, Measurement and Control (1976) 215–223.
[11] J.J. Thomsen, Using fast vibrations to quench friction-induced oscillations, Journal of Sound and Vibration 228 (5) (1999) 1079–1102.
[12] D.M. Tcherniak, Using fast vibration to change nonlinear properties of mechanical systems, Proceedings of IUTAM/IFToMM Symposium in Synthesis of Nonlinear Dynamical Systems, Riga, Latvia, 24–28 August 1998, pp. 227–236.
[13] M.Z. Kolovskij, Influence of fast-frequency excitation to resonant oscillations in nonlinear systems, Truchy Leningradskogo, Plitechiceskogo Institute 226 (1963) 7–17.
[14] I.I. Blekhman, Forming the properties of nonlinear mechanical systems by means of vibration, Proceedings of IUTAM/IFToMM Symposium in Synthesis of Nonlinear Dynamical Systems, Riga, Latvia, 24–28 August 1998, pp. 1–11.
[15] D.M. Tcherniak, J.J. Thomsen, Slow effects of fast harmonic excitation for elastic structures, Nonlinear Dynamics 17 (3) (1998) 227–246.

[16] D.M. Tcherniak, The influence of fast excitation on a continuous system, Journal of Sound and Vibration 227 (2) (1999) 343–360.
[17] M.H. Hansen, Effect of high-frequency excitation on natural frequencies of spinning discs, Journal of Sound and Vibration 234 (4) (2000) 577–589.
[18] J.S. Jensen, Buckling of an elastic beam with added high-frequency excitation, International Journal of Non-Linear Mechanics 35 (2) (2000) 217–227.
[19] J.S. Jensen, D.M. Tcherniak, J.J. Thomsen, Stiffening effects of high-frequency excitation: experiments for an axially loaded beam, American Society of Mechanical Engineers, Journal of Applied Mechanics 67 (2) (2000) 397–402.
[20] J.S. Jensen, Fluid transport due to non-linear fluid-structures interaction, Journal of Fluid and Structures 11 (1) (1997) 327–344.
[21] J.S. Jensen, Articulated pipes conveying fluid pulsating with high-frequency, Nonlinear Dynamics 19 (2) (1999) 173–193.
[22] J.J. Thomson, Vibration induced displacement using high-frequency resonators, and friction layers, Proceedings of the IUTAM/IFToMM Symposium on Synthesis of Nonlinear Dynamical Systems, SNDS '98, Riga Latvia, 24–28 August 1998, pp. 237–246.
[23] A. Fidlin, J.J. Thomsen, Predicting vibration-induced displacement for a resonant friction slider, European Journal of Mechanics A/ Solids 20 (2001) 155–166.